

CEX-58.2

CIVIL EFFECTS EXERCISE

THE SCATTERING OF THERMAL RADIATION
INTO OPEN UNDERGROUND SHELTERS

T. P. Davis, N. D. Miller, T. S. Ely,
J. A. Basso, and H. E. Pearse

20050916 238

Issuance Date: October 30, 1959

CIVIL EFFECTS TEST OPERATIONS

BEST AVAILABLE COPY

Ince 5

NOTICE

This report is published in the interest of providing information which may prove of value to the reader in his study of effects data derived principally from nuclear weapons tests.

This document is based on information available at the time of preparation which may have subsequently been expanded and re-evaluated. Also, in preparing this report for publication, some classified material may have been removed. Users are cautioned to avoid interpretations and conclusions based on unknown or incomplete data.

PRINTED IN USA

Price \$0.75. Available from the Office of
Technical Services, Department of Commerce,
Washington 25, D. C.

THE SCATTERING OF THERMAL RADIATION INTO OPEN UNDERGROUND SHELTERS

By

T. P. Davis, N. D. Miller, T. S. Ely,
J. A. Basso, and H. E. Pearse

Approved by: R. L. CORSBIE
Director
Civil Effects Test Operations

Atomic Energy Project, University of Rochester
Rochester, New York
May 1959

ABSTRACT

Animals placed in open underground shelters at the Nevada Test Site during an atomic weapon test suffered skin burns of an unknown origin. From a study of the burns, the following deductions were made: (1) the causative agent entered the shelter from outside; (2) the causative agent was subject to rectilinear propagation near the entrance; and (3) the causative agent required a relatively unobstructed opening to effect entrance.

The two most likely agents for such burns are (1) hot winds and/or hot wind-borne dust that are forced into the shelter as the shock front from the weapon passes the shelter entrances and (2) radiant energy from the fireball that is scattered into the shelter.

The purpose of this study was to evaluate the contribution made by radiant energy and, if this contribution proved to be significant, to suggest means of eliminating it. The following procedure was adopted: (1) extensive measurements were made in the laboratory on a scale model of the shelter and (2) direct measurements were made on an actual shelter to ensure the validity of the laboratory results.

A Photronic cell and a MacBeth Illuminometer were used to measure the entryway transmission of total radiant energy.

The consistency of the results with extended and point sources for the model shelter and the agreement of these results with those from a point source and sunlight for the underground shelter at the Nevada Test Site lead to considerable confidence in the ability to predict the amount of radiant energy that would reach the animals from a weapon of known size. The energy calculated on the basis of these static measurements is about $\frac{1}{200}$ of that required to produce the burns. Although transient effects caused by the rapid heating of the entryway walls could have resulted in a considerable increase in the entryway transmission, it is felt that radiant energy was neither the sole causative agent nor the most important causative agent in producing burns within the shelters. Hot winds and/or hot wind-borne dust are now considered to be the most likely agents.

ACKNOWLEDGMENTS

The authors would like to acknowledge the enthusiastic encouragement of R. L. Corsbie in the prosecution of this study and the outstanding support provided by the Civil Effects Test Organization during the field phase of the investigation.

It is a pleasure to acknowledge also the invaluable assistance of Harold S. Stewart, formerly with the Naval Research Laboratory and now with the Institute of Optics of the University of Rochester. Dr. Stewart originally suggested the use of scale models for the laboratory studies and made numerous suggestions regarding the design of the field experiments.

To all others, both at the University of Rochester and at the Nevada Test Site, who assisted in these studies, the authors express their thanks and appreciation.

CONTENTS

ABSTRACT	5
ACKNOWLEDGMENTS	6
CHAPTER 1 INTRODUCTION	9
CHAPTER 2 DEVELOPMENT OF PROCEDURE	10
CHAPTER 3 MODEL STUDIES	11
3.1 Surface Characteristics of Concrete and of the Model Materials	11
3.2 Apparatus for Illuminance Measurements in the Shelter Model	12
3.3 Instrumentation for Illuminance Measurements	12
3.4 Results of Illuminance Measurements on the Model	12
3.5 Analysis of Results	15
3.6 Conclusions	18
CHAPTER 4 FIELD STUDIES.	19
4.1 Source	19
4.2 Photoelectric Photometer	19
4.3 Reflectance of Concrete	20
4.4 Results of the Field Studies	21
4.5 Measurements with Point Source	21
4.6 Measurements with Sunlight	24
CHAPTER 5 CONCLUSIONS	26

ILLUSTRATIONS

CHAPTER 3 MODEL STUDIES	
3.1 A Simple Gonio-photometer for Measuring the Diffusion Characteristics of the Surfaces Considered for the Shelter Model	13
3.2 Reflection Characteristics of Several Surfaces Shown as Percentage of Deviation from a Perfect Diffuser for Normal Incidence	13
3.3 Cardboard Model of the Underground Shelter Showing the Tilted Ground Line and the Simulated Fireball	14
3.4 View of the Cardboard Shelter Model Showing the Point-source Housing in Position and the Ring of Lights That Were Used to Illuminate the Fireball	14

ILLUSTRATIONS (Continued)

3.5	Ratio of Illuminance at the Indicated Positions in the Model to Illuminance at the Center of the Model Aperture Measured Normal to the Model Source Axis as a Function of the Reflection Factor of the Interior	16
3.6	Schematic Diagram of the Light from the Point Source Falling on the Plane of the Shelter Aperture and the Principal Rays Used in the Derivation of the Average Flux Correction	18

CHAPTER 4 FIELD STUDIES

4.1	Circuit Diagram	20
4.2	Illumination in the Shelter as a Function of the Reflection Factor (R) of the Interior	23
4.3	Spectral Reflectance of Paints Used in Model Studies and in Field Tests	25

TABLES

CHAPTER 3 MODEL STUDIES

3.1	Ratios of Illuminances at Model Surfaces to Illuminance at Center of Model Aperture (Extended Source)	17
3.2	Ratios of Illuminances at Model Surfaces to Illuminance at Center of Model Aperture (Point Source)	17

CHAPTER 4 FIELD STUDIES

4.1	Ratios of Illuminance at Walls to Average Illuminance at Plane of Shelter Aperture (Field Tests with 2-kw Lamp).	22
4.2	Ratios of Illuminance at Walls to Average Illuminance at Plane of Shelter Aperture (Field Tests)	22
4.3	Ratios of Illuminance at Walls to Average Illuminance at Plane of Shelter Aperture (Model Studies)	24

Chapter 1

INTRODUCTION

The occurrence of skin burns on animals placed in open-entry underground shelters in several field tests of atomic weapons has raised a question as to the mode of heat transfer involved. A consideration of the burns themselves can afford some help in answering this question. Two observations seem most pertinent:

(1) The burns were of a distinctive profile type; i.e., they were confined to surfaces oriented normal to shelter entrances.

(2) Burns were restricted to animals adjacent to relatively unobstructed fast-fill entrances. Animals near partially obstructed slow-fill entrances were not burned.

From these observations the following deductions can be made: (1) the causative agent enters the shelter from outside (this probably rules out the idea that air temperatures within the shelter are raised to damaging values simply by adiabatic, or partially adiabatic, compression); (2) the causative agent is subject to rectilinear propagation near the entrances; and (3) the causative agent requires a relatively unobstructed opening to effect entrance.

The two most likely agents are (1) hot winds and/or hot wind-borne dust that are forced into the shelter as the shock front from the weapon passes the shelter entrances and (2) radiant energy from the fireball that is scattered into the shelter. Obviously, these two agents, plus adiabatic heating, plus other unsuspected factors, are operating simultaneously or in rapid sequence, and the burn is probably the resultant of this complex of hyperthermic insults.

The elimination of the burn hazard in shelters depends upon a separate, systematic investigation of each suspected agent. The purpose of the present investigation was to evaluate the contribution made by radiant energy and, if such contribution proved to be significant, to suggest means of eliminating this component.

Chapter 2

DEVELOPMENT OF PROCEDURE

A calculation of the radiant energy incident upon a surface located within a shelter requires a knowledge of (1) the total radiant energy and its polar distribution at the exterior of the shelter entrance and (2) the entryway transmission factor. A reasonable estimate of the former can be obtained by extrapolation from calorimetric measurements on similar sources and from the test configuration. Since the arrival of the shock wave at the shelter brings an opaque dust cloud that blocks any further reception of radiation from the weapon, the time of arrival of the shock wave must be known. Local "pop-corning" and other transient phenomena are unpredictable and introduce some doubt into these estimates.

The entryway transmission factor depends upon the reflectance of the entrance walls, the geometry of the entryway, and the orientation of the entrance with respect to the weapon. Originally, it was suggested that the most feasible method of evaluating this factor was by direct measurement in an actual shelter with a steady source, such as a tungsten lamp, and a sensitive receiver. Such a procedure, however, would not provide proper simulation of test geometry. In an actual atomic weapon test the conditions were that of an approximately $f/1.0$ system. These conditions could not be adequately represented by the essentially point-source optics originally suggested.

The following operational approach was finally adopted as one that would probably yield reliable results. With a scale model it would be relatively simple to secure a good approximation to atomic weapon test geometry through the use of a reasonably sized extended source. Then, if the results from this extended source were compared with results obtained using the scale model and a point source, a geometry factor would be found. This factor could then be applied to measurements with a point source made in the field on an actual shelter to correct field results to the geometry applicable to an atomic weapon test situation. Thus the field measurements made with a point source would be used to validate the laboratory measurements made with a point source on the model. This, in fact, was the principal purpose of the field measurements, which indicates the importance of the model studies. This emphasis on the latter studies was altogether desirable since it removed the most critical measurements from the field to the more suitable laboratory environment.

An additional problem, basically even more difficult than that of geometry, concerns the transient phenomena occurring in the entryway during the thermal pulse. It is pointed out later in this report that this remains an unresolved problem since the measurements reported herein are, by necessity, static and do not reflect these transient effects.

Chapter 3

MODEL STUDIES

The behavior of light from either an extended source or a point source in a typical open underground shelter was studied in the laboratory with a cardboard scale model constructed from blueprints of an actual shelter. The extended source was a uniformly illuminated disk, 8 ft in diameter, placed 8.4 ft in front of the model. This provided an $f/1.16$ system, which corresponded to the geometry of a fireball in field tests. A 100-watt coiled-filament projection lamp was used for the point source. A MacBeth Illuminometer was used to measure the illuminance on the walls within the model. Measurement was accomplished by punching small ports in the cardboard just large enough to allow the sighting tube of the instrument to be slipped in to view the opposite surface. The attenuation of light at various points in the shelter was calculated by dividing the value of illuminance at each such point by that incident at the plane of the shelter entrance.

As mentioned above, the entryway transmission depends also on the reflectance of the entrance walls. It was suggested that this relation might follow an empirical extension of integrating sphere theory. In a simple integrating sphere, the illuminance at the interior surface is directly proportional to the ratio $R/(1-R)$, where R is the reflectance of the surface. Since it seemed likely that various portions of the shelter entryway would act as partial integrating spheres, it was hypothesized that the illuminance at any point on a wall of the structure would depend upon reflectance as $[R/(1-R)]^a$, where the exponent, a , could take on any positive value. This hypothesis was investigated by painting the inside of the model with four different mixtures of black and white paint. This provided four reflection factors with similar diffusion and spectral characteristics. Measurements of illuminance were made at 30 points in the model for the highest reflectivity and at about half that many for the darkest gray.

3.1 SURFACE CHARACTERISTICS OF CONCRETE AND OF THE MODEL MATERIALS

It was necessary to duplicate the shelter geometry by accurate scaling and to reproduce the diffusing properties of the walls as closely as possible so that the model studies would be meaningful in terms of field tests. The concrete walls of the actual shelter are reasonably good Lambert surfaces; i.e., the intensity of the light reflected at any angle from the normal to the surface is nearly equal to the intensity along the normal times the cosine of the angle. There is some increase in the intensity at grazing angles of incidence and reflection, but with dry concrete this error is small. Therefore it was desirable to approximate closely a Lambert surface for the walls of the model. The white Bristol board used in the construction of the model showed a large error at nearly grazing angles of incidence; therefore it was necessary to find a coating for the wall that would provide good diffusion.

An instrument was constructed in the laboratory to measure the intensity of the reflected beam at any angle from the normal for any angle of incidence (see Fig. 3.1). It consisted of a collimated light source (S) clamped on the periphery of a graduated circle (C) mounted on a rotating table. A sample holder (H) was provided in the center of the table which allowed the sample to be illuminated at a fixed angle as it rotated about the axis of the graduated circle.

A MacBeth Illuminometer (M) was clamped in a fixed position to the bench with its optical axis aimed at the center of rotation of the sample.

Several samples of paint and a surface chip of concrete were measured in this way. The results are presented in Fig. 3.2, which shows the per cent deviation from the cosine law for normal incidence. The Prang show-card paint provided the closest approach to a Lambert surface for the model walls. The mixtures of black and white paint provided good neutral grays to approximate the spectral reflectance of a concrete surface.

3.2 APPARATUS FOR ILLUMINANCE MEASUREMENTS IN THE SHELTER MODEL

In the field the underground shelter received thermal radiation from a fireball, the center of which was 25.5 deg above the ground level. The objective was to simulate these field conditions as accurately as possible in the laboratory with visible light so that the attenuation of the thermal radiation at any point inside the shelter could be determined by extrapolation. The Division of Biology and Medicine, USAEC, provided blueprints of the shelter from which a 1:10 scale model was constructed.

It can be demonstrated rigorously that a diffuse luminous sphere can be replaced by a flat disk having a Lambert surface set normal to the line of sight to the center of the sphere. The dimensions of the laboratory restricted the size of the source and its distance from the model; so the 1:10 scale for the illuminated disk could not be maintained. The diameter and distance were changed proportionately so that the solid angle subtended at the center of the model aperture could be kept the same as in the field tests with the nuclear weapon.

The fireball was simulated by suspending from the ceiling beams an 8-ft square of plywood on which a circle was inscribed with white Prang show-card paint. The corners of the square were painted flat black, and heavy black velour drapes were hung to prevent light scattered from the walls and ceilings from reaching the model. The white disk was illuminated by a ring of lights set in a board with an opening in the center large enough to allow the model to "see" the whole disk. The ground level of the system was tilted up 25.5 deg so that the disk could be hung vertically and the model would be at a comfortable working height. The arrangement is shown in Figs. 3.3 and 3.4.

Figure 3.4 also shows the location of the light for the point source. In anticipation of field tests with a 2-kw lamp, this 100-watt projection lamp was placed near the end of the approach to the first stair well since this position would ensure that the aperture would be filled with light and yet would give an illumination level high enough for field measurements. The lamp was placed on the axis defined by the center of the shelter entrance and the center of the extended source.

3.3 INSTRUMENTATION FOR ILLUMINANCE MEASUREMENTS

The MacBeth Illuminometer is a visual instrument, which uses a standard lamp operated on dry-cell batteries with a controlled current to illuminate a comparison field, the luminance of which is altered by changing the position of the lamp relative to a diffusing screen in the field. This allows the luminance of the comparison field to be adjusted to match that of the sample surface. The sample and comparison fields are seen as concentric circles. Calibration for any type of diffuse surface can be accomplished by changing the current through the standard lamp to produce a match with a reference standard of known illuminance on the surface. Through the use of neutral-density filters in either the comparison or sample fields a range of from 1.5×10^{-3} to 2.0×10^4 ft-c can be measured. The sighting aperture of the instrument was slipped into the ports cut in the model walls for the measurements. Plugs of the same diameter as the ports were made and painted with the walls. These were used in all ports except the one being used for measurement; so the whole unit was lighttight.

3.4 RESULTS OF ILLUMINANCE MEASUREMENTS ON THE MODEL

The reflection factor for a chip of concrete from the shelter wall was 36.8 per cent for visible light. So that the value of 0.6 for its $R/(1-R)$ factor would be bracketed, four paint

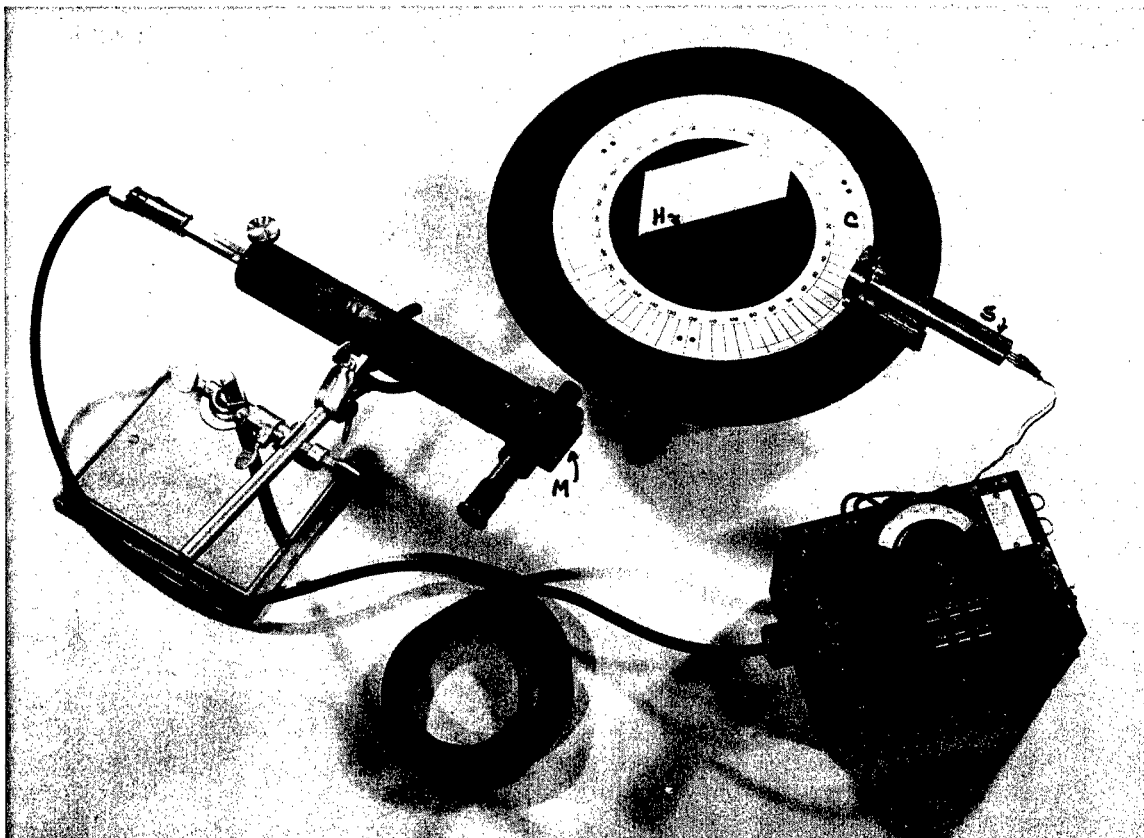


Fig. 3.1—A simple gonio-photometer for measuring the diffusion characteristics of the surfaces considered for the shelter model.

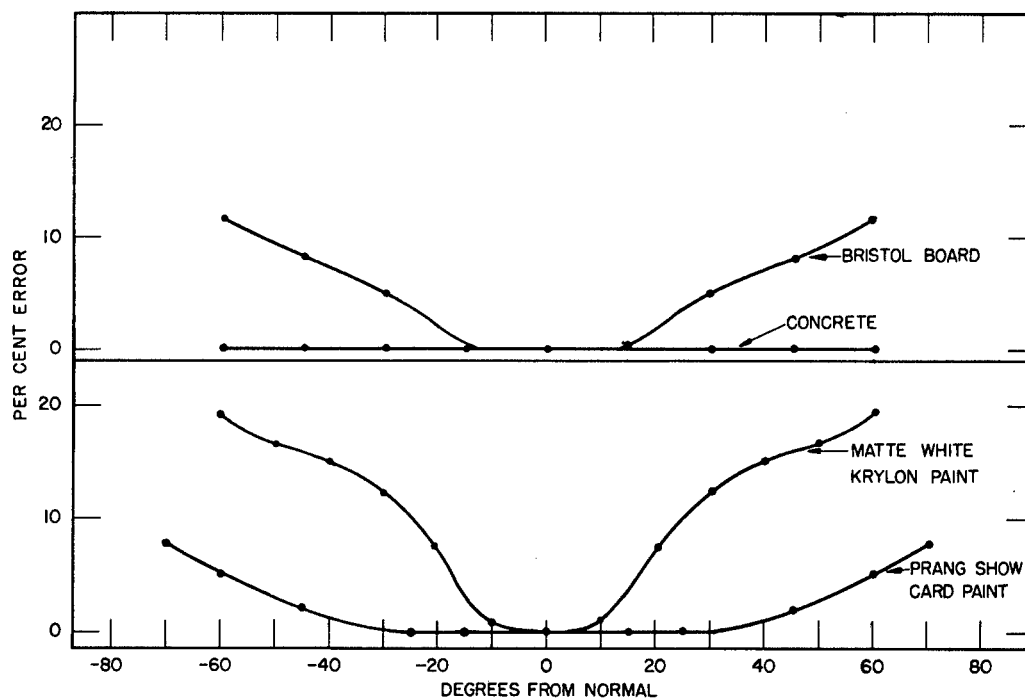


Fig. 3.2—Reflection characteristics of several surfaces shown as percentage of deviation from a perfect diffuser for normal incidence.

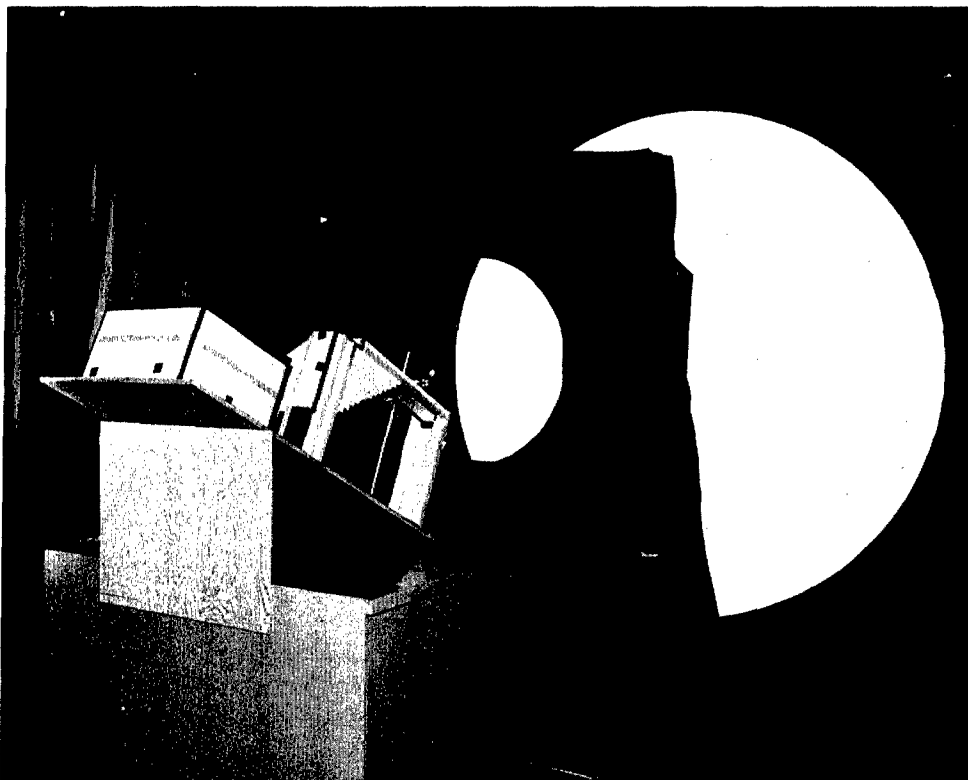


Fig. 3.3—Cardboard model of the underground shelter showing the tilted ground line and the simulated fireball.

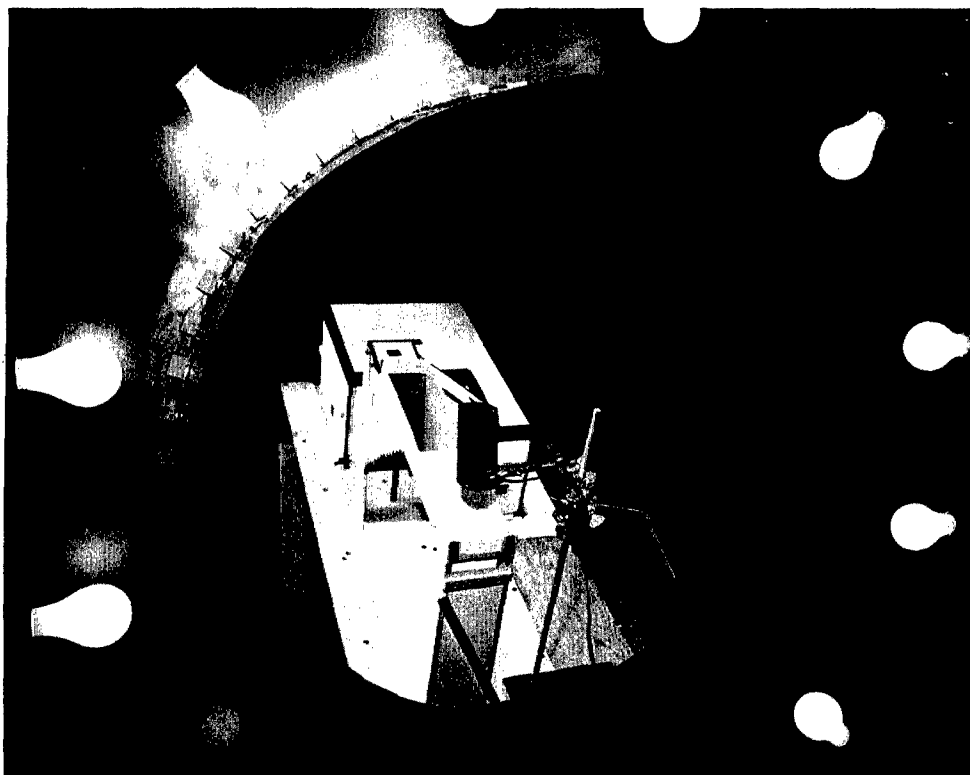


Fig. 3.4—View of the cardboard shelter model showing the point-source housing in position and the ring of lights that were used to illuminate the fireball.

mixtures were used, yielding reflection factors of 20.4, 39.2, 67.7, and 86.1 per cent. This gave a range of $R/(1-R)$ values from 0.26 to 6.2. Both the $f/1.16$ extended source and the point source were used to illuminate the model for each of these paints on the interior walls and surfaces. For each condition of model interior and source, measurements of illuminance were made at the center of the model entrance and at as many ports as practicable. The ratios of the illuminance at each port to that at the aperture center of the model were calculated. Values are tabulated for 18 representative points in the model for the extended source (Table 3.1) and for the point source (Table 3.2), with a description of the position in the shelter to which they apply.

In Fig. 3.5 the logarithm of the ratio of illuminance at the entrance of the fast-fill room to the illuminance at the center of the model aperture is plotted against $\log [R/(1-R)]$. The four points for each source fall on a reasonably straight line, indicating the soundness of the integrating-sphere approach. The slope of the straight lines drawn as the best fit through the points for each source is approximately 2, which implies that the shelter from the entrance through stair wells and corridor to the entrance to the fast-fill room is acting as two integrating spheres. Similar illuminance ratios for two other locations in the shelter are also plotted in Fig. 3.5. The slopes of the plots for all measured positions vary from 0.3 to 2.

3.5 ANALYSIS OF RESULTS

The lines in Fig. 3.5 that are the best fit to the data for the two sources used are displaced by a nearly constant amount for each of the positions in the model. The plotted points are the ratios of the measured illuminances at different positions to the illuminance on a card placed normal to the center line of the source passing through the center of the model aperture. This reference point was chosen on the assumption that it would give the average value of illuminance over the plane of the entrance. In the case of the point source, a more careful analysis of the true condition provides an explanation for the displacement of the two sets of curves describing the attenuation of radiation for the two sources.

The distance from the point source to the opening of the stair well, L_1 , is much shorter than the distance to the end of the aperture, L_2 (Fig. 3.6). The angles between these two lines and the normal to the plane of the entrance (through the top step and the ceiling of the landing) are also quite different. The radiant energy passing through an increment of that plane will be inversely proportional to the square of the distance and will vary with the cosine of the angle. Therefore the average illuminance across the aperture will not equal that at the center; for the dimensions of our system, it will be 1.21 times the value measured at the center. This factor can be applied to all but the 67.7 per cent paint mixture, where the point source was placed 1.18 ft away and 24 deg from the entry plane. The correction factor in this case is 1.06. The correction for the extended source is negligible because of the greater distance to the disk. The ratios shown in Table 3.1 were corrected by the above factors before being plotted with the extended source data in Fig. 4.2.

An effort was made to calculate the component of direct illumination on the head wall for the two sources and to check it with direct measurements. The direct measurement of this quantity for the extended source is found by subtracting the illuminance at the ceiling of the first landing (which receives no direct illumination from the disk) from the illuminance at the head wall. The area of the disk that could be seen from the port of the head wall was found by projecting the aperture of the model onto the disk with a small source in the port. The area of the illuminated trapezoid on the simulated bomb was 12.9 sq ft. This area would produce an illuminance at the head wall 0.216 times as great as the full area of the simulated bomb. The measured values of direct illuminance for the four paint mixtures were:

86.1%	67.7%	39.2%	20.4%
0.215	0.225	0.224	0.246

The direct component for the point source is given simply by the square of the ratio (distance from source to aperture center)/(distance from source to head wall). This ratio, when multiplied by the cosine of the angle between the normal to the wall and the line of the source, is

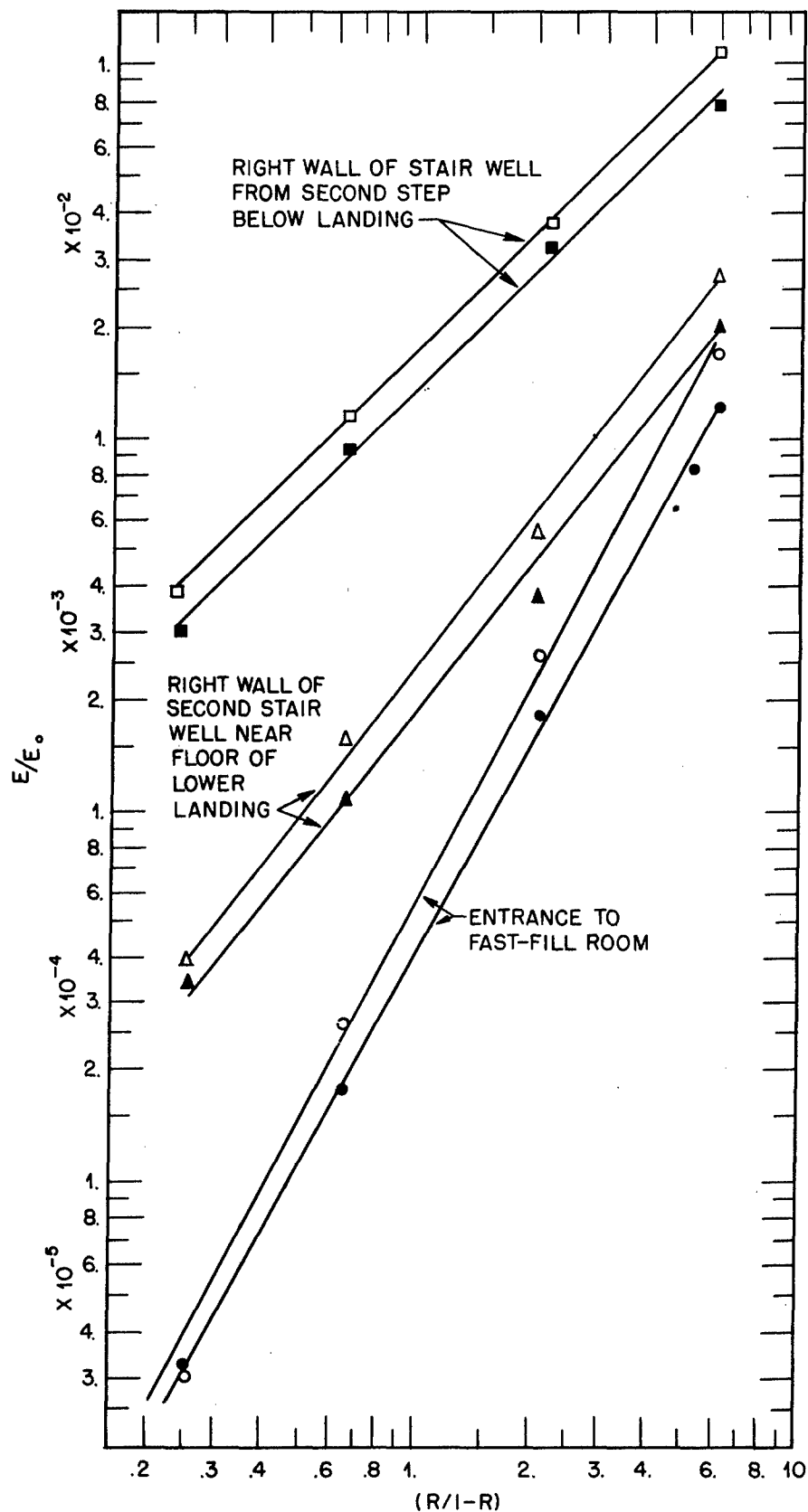


Fig. 3.5—Ratio of illuminance at the indicated positions in the model to illuminance at the center of the model aperture measured normal to the model source axis as a function of the reflection factor of the interior. ■▲●, extended source. □△○, point source.

TABLE 3.1—RATIOS OF ILLUMINANCES AT MODEL SURFACES TO ILLUMINANCE
AT CENTER OF MODEL APERTURE (EXTENDED SOURCE)

Location in terms of actual shelter	A*	B*	C*	D*
Head wall of first stair well 5 ft above landing floor	3.44×10^{-1}	2.94×10^{-1}	2.55×10^{-1}	2.18×10^{-1}
Head wall of first stair well near ceiling of landing	1.41×10^{-1}	9.81×10^{-2}	5.41×10^{-2}	3.91×10^{-2}
Left wall of first stair well 3 ft above 8th tread	1.93×10^{-1}	1.52×10^{-1}	8.73×10^{-2}	8.86×10^{-2}
Left wall of first stair well 2.2 ft above 11th tread	1.50×10^{-1}	9.74×10^{-2}	4.64×10^{-2}	3.85×10^{-2}
Left wall of first stair well 1 ft above landing floor	1.60×10^{-1}	1.15×10^{-1}	8.85×10^{-2}	2.79×10^{-2}
Floor of first landing	2.26×10^{-1}	1.40×10^{-1}	1.05×10^{-1}	7.09×10^{-2}
Ceiling of first landing	1.20×10^{-1}	6.86×10^{-2}	3.10×10^{-2}	1.44×10^{-2}
Left wall of second stair well 5 ft above 2nd tread	7.95×10^{-2}	3.12×10^{-2}	8.91×10^{-3}	3.00×10^{-3}
Right wall of second stair well 5 ft above 2nd tread	7.70×10^{-2}	3.54×10^{-2}	1.14×10^{-2}	
Ceiling of second stair well over 2nd tread	1.32×10^{-1}	6.65×10^{-2}	2.62×10^{-2}	
Ceiling of second stair well over 7th tread	6.41×10^{-2}	2.19×10^{-2}	7.55×10^{-3}	
Right wall of second stair well 1.5 ft above landing floor	1.97×10^{-2}	3.71×10^{-3}	1.05×10^{-3}	3.45×10^{-4}
Wall at end of second stair well 1 ft above landing floor	2.48×10^{-2}	5.48×10^{-3}	1.73×10^{-3}	5.36×10^{-4}
Wall at end of second stair well 6.5 ft above floor	3.42×10^{-2}	1.03×10^{-2}	3.09×10^{-3}	1.18×10^{-3}
Right wall halfway through corridor 2 ft above floor	9.40×10^{-3}	1.67×10^{-3}	2.73×10^{-4}	
Entrance to fast-fill room 2 ft above floor	1.23×10^{-2}	1.81×10^{-3}	1.73×10^{-4}	3.18×10^{-5}
Wall of fast-fill room directly opposite entrance	1.62×10^{-3}	2.46×10^{-4}	3.09×10^{-5}	
Floor in center of fast-fill room	1.29×10^{-3}			

*Reflection factor and R/(1-R) value, respectively, are: A, 86.1 per cent and 6.2; B, 67.7 per cent and 2.1; C, 39.2 per cent and 0.65; and D, 20.4 per cent and 0.26.

TABLE 3.2—RATIOS OF ILLUMINANCES AT MODEL SURFACES TO ILLUMINANCE
AT CENTER OF MODEL APERTURE (POINT SOURCE)

Location in terms of actual shelter	A*	B*	C*	D*
Head wall of first stair well 5 ft above landing floor	4.15×10^{-1}	3.14×10^{-1}	3.15×10^{-1}	2.87×10^{-1}
Head wall of first stair well near ceiling of landing	1.30×10^{-1}	5.36×10^{-2}	2.11×10^{-2}	9.02×10^{-3}
Left wall of first stair well 3 ft above 8th tread	2.20×10^{-1}	1.47×10^{-1}	1.08×10^{-1}	8.47×10^{-2}
Left wall of first stair well 2.2 ft above 11th tread	1.94×10^{-1}	1.03×10^{-1}	6.36×10^{-2}	4.78×10^{-2}
Left wall of first stair well 1 ft above landing floor	1.98×10^{-1}	1.27×10^{-1}	9.88×10^{-2}	5.27×10^{-2}
Floor of first landing	3.71×10^{-1}	2.52×10^{-1}	2.46×10^{-1}	1.70×10^{-1}
Ceiling of first landing	1.57×10^{-1}	7.36×10^{-2}	2.31×10^{-2}	1.42×10^{-2}
Left wall of second stair well 5 ft above 2nd tread	1.00×10^{-1}	3.30×10^{-2}	1.19×10^{-2}	3.85×10^{-3}
Right wall of second stair well 5 ft above 2nd tread		4.30×10^{-2}	1.82×10^{-2}	
Ceiling of second stair well over 2nd tread	1.64×10^{-1}	6.88×10^{-2}	3.54×10^{-2}	
Ceiling of second stair well over 7th tread	9.27×10^{-2}	2.83×10^{-2}	1.20×10^{-2}	
Right wall of second stair well 1.5 ft above landing floor	2.74×10^{-2}	5.52×10^{-3}	1.52×10^{-3}	3.93×10^{-4}
Wall at end of second stair well 1 ft above landing floor	3.20×10^{-2}	6.85×10^{-3}	2.19×10^{-3}	6.01×10^{-4}
Wall at end of second stair well 6.5 ft above floor	5.21×10^{-2}	1.30×10^{-2}	4.59×10^{-3}	1.54×10^{-3}
Right wall halfway through corridor 2 ft above floor	1.37×10^{-2}	1.59×10^{-3}	2.05×10^{-4}	2.73×10^{-5}
Entrance to fast-fill room 2 ft above floor	1.68×10^{-2}	2.63×10^{-3}	2.65×10^{-4}	3.06×10^{-5}
Wall of fast-fill room directly opposite entrance	2.00×10^{-3}	2.00×10^{-4}	2.95×10^{-5}	
Floor in center of fast-fill room	1.67×10^{-3}	1.01×10^{-4}		

*Reflection factor and R/(1-R) value, respectively, are: A, 86.1 per cent and 6.2; B, 67.7 per cent and 2.1; C, 39.2 per cent and 0.65; and D, 20.4 per cent and 0.26.

0.277. The measured values in this case are found by subtracting the measurement at the top of the head wall near the ceiling from the reading taken above the landing floor. They are:

86.1%	67.7%	39.4%	20.4%
0.285	0.278	0.294	0.278

The agreement between calculated and measured values of the direct radiation is very encouraging and points the way to further analysis of the data. In some portions of the model, the

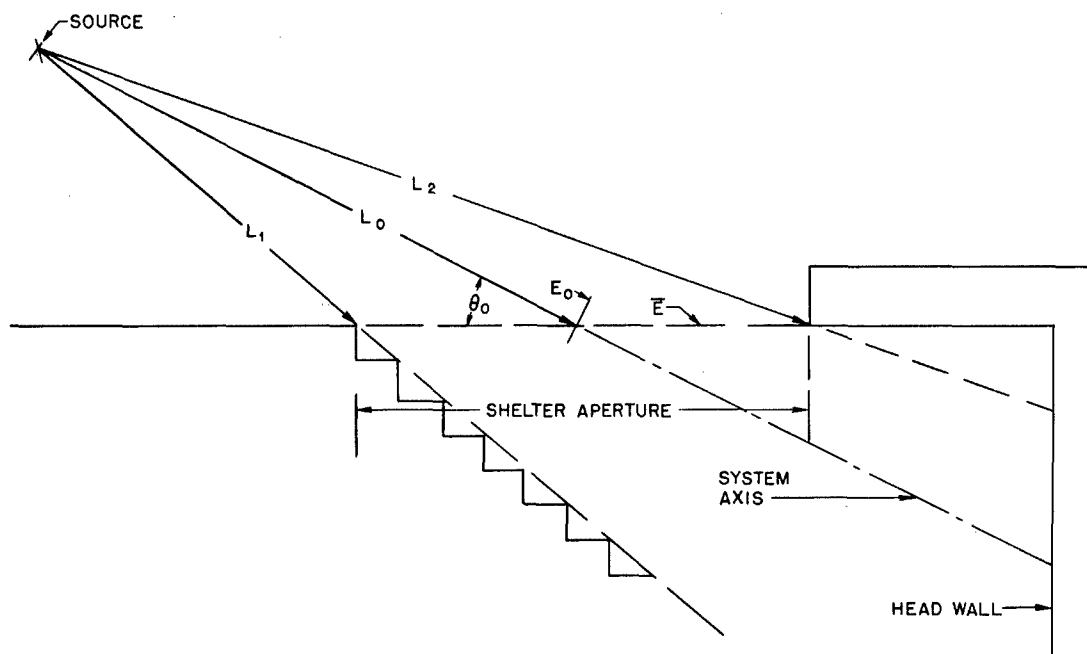


Fig. 3.6—Schematic diagram of the light from the point source falling on the plane of the shelter aperture and the principal rays used in the derivation of the average flux correction. $E_0 = I/L_0^2$; $E_{av} = E_0 L_0 \left[\frac{L_1 + L_2}{(L_1 L_2)^{1/2}} \right]$; $\bar{E} = E_{av} \sin \theta_0$; E_{av} = average value of illuminance normal to system axis across shelter aperture; \bar{E} = average illuminance at plane of the shelter aperture.

strong first reflections can be calculated from the bright wall producing them. Agreement with measured values in this case is equally good. This method of calculation would be of value in any redesign of the structure when such secondary sources might be of interest.

3.6 CONCLUSIONS

It seems probable, on the basis of the model studies, that the level of illumination at any point inside a shelter can be predicted if the average illuminance at the plane of the opening of the stair well is known. At least from the present studies, this prediction can be made for a source near the horizon on the axis of the first stair well. The agreement between the point and extended sources, after due care was taken in finding the average illuminance values across the opening, was quite remarkable. This greatly increased the confidence in the field studies with a point source on the full-scale shelter.

Chapter 4

FIELD STUDIES

Measurements of light attenuation in shelters were continued on the full-scale structures at the Nevada Test Site. All participants in this exercise assembled at the Test Site on Aug. 18, 1958. The available shelters (in Areas 1 and 4) were immediately inspected, and all equipment was uncrated and checked. On Aug. 19, the equipment was moved to the Forward Area and installed in the shelter in Area 1; at the same time the Area 4 shelter was painted. Measurements were made in the Area 1 shelter through the night of Aug. 19, and the equipment was then transferred to Area 4; the vacated shelter was then painted. Measurements in the Area 4 shelter were made the night of Aug. 20, and a final set of readings was taken in the Area 1 shelter during the night of Aug. 21. These readings were made at night so that the only illumination in the shelter would come from the carefully placed point source. The moon was between new (Aug. 14) and first quarter (Aug. 21); so there was no interference from it.

All measurements employing a point source were made with two completely independent receiver systems, the MacBeth Illuminometer, previously described, and a photoelectric photometer, described in Sec. 4.2. One additional set of measurements was made on the afternoon of Aug. 21, with the brilliant sunlight and skylight supplying the illumination. The MacBeth Illuminometer only was used for these measurements.

4.1 SOURCE

The point source of light was a 2000-watt tungsten spotlight lamp, carrying the General Electric designation 2M/T30/1 and rated at approximately 48,000 total initial lumen output. The concentrated filament of this lamp was placed at the center of curvature of a spherical second-surfaced reflector, which increased the flux in the forward direction about 20 per cent. The lamp and reflector were mounted in a simple enclosure provided with a blower for cooling, a panel-mounted voltmeter for measuring voltage across the lamp, and a simple vane shutter. (This unit is a medium-intensity burning source with the condenser lenses removed.)¹ The housing was securely mounted on a heavy camera tripod, giving simple control of elevation and tilt. The source was placed on the system axis, extending from the design center point of the shelter entrance to the center of burst (former tower cab) and at a slant range of 10.8 ft from the former point.

4.2 PHOTOELECTRIC PHOTOMETER

The primary receiving element was a Weston Photronic barrier-layer photocell, model 856 RR. This unit has a design sensitivity of $4 \mu\text{a}/\text{ft-c}$, with a spectral sensitivity limited to the visible region of the spectrum. It was necessary to measure cell currents from a maximum of about $300 \mu\text{a}$ with the cell at the center of the shelter entrance to a minimum of about $10^{-3} \mu\text{a}$ with the cell on the floor of the shelter.

The circuit² selected for these measurements is shown in Fig. 4.1. The principle of the circuit is a null current balance. An exact analysis demonstrates that, when the galvanometer

indicates a null balance, then

$$I_{s.c.} = I_M \frac{R_2}{R_1 + R_2}$$

where $I_{s.c.}$ is the cell short-circuit current (the current delivered by the cell to a zero-resistance external circuit) and I_M is the meter current. The components were as follows:

Cell = Weston Photronic model 856 RR; sensitivity, $4 \mu\text{a/ft-c}$

G = Honeywell electronic null indicator; sensitivity, 10^{-8} amp/division; input resistance, 1000 ohms

I = Rawson microammeter, multi-range, 50/100/200/500/1000 μa full scale; 100 ohms resistance on all ranges; accuracy, ± 0.5 per cent of full scale on any range

$R_1 - R_2$ = Leeds & Northrup Co., Ayrton shunt, with $R_1 + R_2 = 40,000$ ohms and $[R_2/(R_1 + R_2)]$ ratios of 1, 10^{-1} , 10^{-2} , 10^{-3} , and $10^{-4} \pm 0.1$ per cent

A $1\frac{1}{2}$ -volt dry cell was adequate for the aiding battery with a 6-dial decade box used for current control.

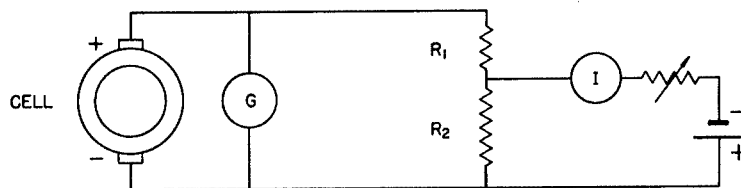


Fig. 4.1—Circuit diagram.

For the most sensitive measurements, R_1 was approximately 40,000 ohms; therefore with slight circuit imbalance, virtually all (approximately 98 per cent) cell current flowed through the null indicator, yielding efficient utilization of the full sensitivity of the indicator. It was possible to predict a receiver-system accuracy of about 3 per cent at the lower limit of illuminance to be measured.

According to manufacturer's data, the linearity of the RR type cell should be excellent over the range 8.6 to 8.6×10^{-3} ft-c. This factor was investigated by the inverse-square method to measure relative response, and the linearity was found to be completely satisfactory.

Finally, it was necessary to investigate the ability of the Photronic cell (and the MacBeth Illuminometer) to measure the entryway transmission of total radiant energy with its sensitivity limited to the narrow region of visible light. Significant errors could be introduced if the entryway walls (concrete) exhibited a markedly nonuniform spectral reflectance.

The model studies indicated that the wall reflectance affects the entryway transmission as $[R/(1-R)]^a$, where R is the total wall reflectance to the wavelength distribution of the incident radiant energy. The Photronic cell could then be considered a suitable receiver if the following condition was met: the diffuse reflectance of concrete to the intended source of radiation as measured by the Photronic cell must be equal to the diffuse reflectance to the same source as measured by a neutral (gray-body) receiver. Measurements, described below, were made on a representative sample of concrete obtained in Rochester and on a core sample of concrete obtained from an NTS shelter.

4.3 REFLECTANCE OF CONCRETE

The diffuse spectral reflectance (total back-scatter) of smooth-surfaced concrete samples was measured using the integrating-sphere reflectometer described by Krolak³ and by Jacquez.⁴ In this instrument the sample is irradiated normally with monochromatic radiation from a Perkin-Elmer model 83 monochromator, and the back-scattered radiation is collected by a magnesium oxide-coated 11.4-cm-diameter integrating sphere. A 10 by 10 mm Eastman Ektron lead sulfide cell is used as a detector, with a Perkin-Elmer preamplifier-amplifier system. The spectral range covered is from 0.4 to 2.6 μ .

Within this range, which includes 86 per cent of the radiation from a 3200°K tungsten lamp, the spectral reflectance of the concrete, R_λ , was nearly constant at about 30 per cent. A thorough analysis of the data yielded the following values:

$$\begin{aligned} R_{\text{cell}} &= 32 \text{ per cent} \\ R_{\text{true}} &= 31 \text{ per cent} \end{aligned}$$

This is a completely insignificant difference; therefore one is assured that the Photronic cell yielded accurate entryway-transmission values with the tungsten-lamp source. Because of the marked neutrality of the concrete spectral reflectance, the same result may be expected to hold for other sources and receivers as well.

4.4 RESULTS OF THE FIELD STUDIES

The first set of measurements was made on the unpainted concrete walls of the Area 1 shelter, which had been washed about one week previous to the tests. The walls were non-uniform with large areas of surface resembling whitewash; direct measurements of reflection factors varied from 0.247 to 0.636. Two more complete sets of measurements were made after the interior of the shelters had been painted with buff paint ($R = 73.8$ per cent) and gray paint ($R = 29.9$ per cent). When the measurements of incident flux at the different positions in the shelter were referred to the average flux at the shelter aperture, as was done in the model studies, the results agreed very well with the laboratory work.

The MacBeth Illuminometer was used with a diffuse test plate of 80 per cent reflectance for measurements on the unpainted shelter and for the two aperture-center measurements made after the shelter had been painted. The interior measurements in the painted shelters were made directly on the wall surfaces after the lamp current had been calibrated to the correct scale values. The agreement between the Illuminometer readings and the Photronic cell short-circuit current remained excellent. The cell was taped to the wall at the desired position, and the sighting aperture of the Illuminometer was directed to an adjacent location. The average values of the readings of the two instruments for the aperture center illumination on the three nights of testing are as follows:

	August 19	August 20	August 21
Cell short-circuit current, μa	311	299	336
Illuminometer, ft-c	62.4	57.4	67.0
Microampere/ft-c	4.99	5.21	5.02

This degree of agreement did not hold throughout the shelter. In some places the Photronic cell was the preferred instrument because it could be taped to the wall and the passage above it left unobstructed. The person holding the Illuminometer, on the other hand, produced fairly effective blocking of the passage in some places. However, there were a few positions where the Illuminometer was the better instrument owing to the fairly large cosine failure of the Photronic cell. These positions were along the walls of the stair wells, where the light struck the cell at a very large angle to the normal. Fortunately, both instruments were at maximum efficiency at the entrance to the fast-fill room.

4.5 MEASUREMENTS WITH POINT SOURCE

The ratios of wall illuminance to the average illuminance at the shelter aperture for six positions in the shelter and for the three conditions of interior surface are recorded in Tables 4.1 and 4.2. The values predicted from the model studies and the values obtained in the field tests with the two different instruments are listed in adjacent columns for comparison. The same values are presented graphically in Fig. 4.2, where the straight lines are the best fit to the model data and the open and closed circles are the results of the field tests. The data from the model studies, corrected for average illuminance at the plane of the aperture, are listed in Table 4.3 for the six shelter locations shown in Fig. 4.2.

TABLE 4.1—RATIOS OF ILLUMINANCE AT WALLS TO AVERAGE ILLUMINANCE
AT PLANE OF SHELTER APERTURE (FIELD TESTS WITH 2-KW LAMP)

Location in terms of actual shelter	Predicted	MacBeth	Photocell
Gray paint [$R/(1-R) = 0.47$]			
Head wall at intersection of system axis	6.0×10^{-1}	7.47×10^{-1}	6.64×10^{-1}
Scattered light on head wall near ceiling	3.0×10^{-2}	2.62×10^{-2}	2.48×10^{-2}
Wall at left of second stairs above 2nd tread	1.5×10^{-2}	1.68×10^{-2}	1.45×10^{-2}
Wall at bottom of second stairs 1 ft above floor	2.5×10^{-3}		2.66×10^{-3}
Entrance to fast-fill room	2.0×10^{-4}	3.18×10^{-4}	2.00×10^{-4}
Floor in center of fast-fill room	5.0×10^{-6}		4.78×10^{-6}
Unpainted concrete [$R/(1-R) = 0.6$]			
Head wall at intersection of system axis	6.2×10^{-1}	6.34×10^{-1}	6.22×10^{-1}
Scattered light on head wall near ceiling	3.5×10^{-2}	2.48×10^{-2}	2.62×10^{-2}
Wall at left of second stairs above 2nd tread	1.8×10^{-2}	1.75×10^{-2}	1.81×10^{-2}
Wall at bottom of second stairs 1 ft above floor	2.9×10^{-3}		3.08×10^{-3}
Entrance to fast-fill room	2.3×10^{-4}	2.30×10^{-4}	4.13×10^{-4}
Floor in center of fast-fill room	7.4×10^{-6}		1.55×10^{-5}

TABLE 4.2—RATIOS OF ILLUMINANCE AT WALLS TO AVERAGE ILLUMINANCE
AT PLANE OF SHELTER APERTURE (FIELD TESTS)
[Buff paint, $R/(1-R) = 2.8$]

Location in terms of actual shelter	Predicted	MacBeth	Photocell
With 2-kw lamp			
Head wall at intersection of system axis	7.6×10^{-1}	7.85×10^{-1}	7.75×10^{-1}
Scattered light on head wall near ceiling	1.5×10^{-1}	1.22×10^{-1}	1.22×10^{-1}
Wall at left of second stairs above 2nd tread	9.6×10^{-2}	1.06×10^{-1}	9.0×10^{-2}
Wall at bottom of second stairs 1 ft above floor	2.4×10^{-3}		2.04×10^{-2}
Entrance to fast-fill room	7.8×10^{-3}	6.19×10^{-3}	5.85×10^{-3}
Floor in center of fast-fill room	4.9×10^{-4}		3.18×10^{-4}
With sunlight			
East wall of first stairs (receiving direct illumination)		6.3×10^{-1}	
Scattered light on head wall		9.09×10^{-2}	
Wall at left of second stairs above 2nd tread		3.92×10^{-2}	
Wall at bottom of second stairs 1 ft above floor		6.8×10^{-3}	
Entrance to fast-fill room		4.2×10^{-3} at 2:31 P.M.; 2.16×10^{-3} at 3:24 P.M.	
Floor in center of fast-fill room		1.29×10^{-4} at 3:22 P.M.	

The pitfalls in photometry are many, and the usual figure stated for the accuracy of MacBeth Illuminometer measurements is 3 to 5 per cent. Since each value presented is a ratio of two illuminance levels, the error is doubled. In the field tests the 2-kw lamp was powered by a gasoline generator, and, although the voltage input was constantly monitored, the luminous output of an incandescent lamp fluctuates so widely for very small changes in voltage that a 10 per cent variation in candle power is probably a conservative estimate of the fluctuations. Add to this variation the presence of light-intoxicated desert insects, which frequently swarmed across the lamp beam, and the variation may have been closer to 20 per cent.

The nonuniformity of the natural concrete in the first field test made it difficult to arrive at an accurate estimate of the $R/(1-R)$ ratio. The buff and gray interior paints removed this obstacle, however, and provided very uniform reflecting surfaces. The spectral reflectance curves of these two paints were measured at Eastman Kodak Research Laboratories from sample chips painted at the same time the walls were painted. The curves are reproduced in Fig. 4.3 along with the curves from the Prang show-card paint used in the model studies. The

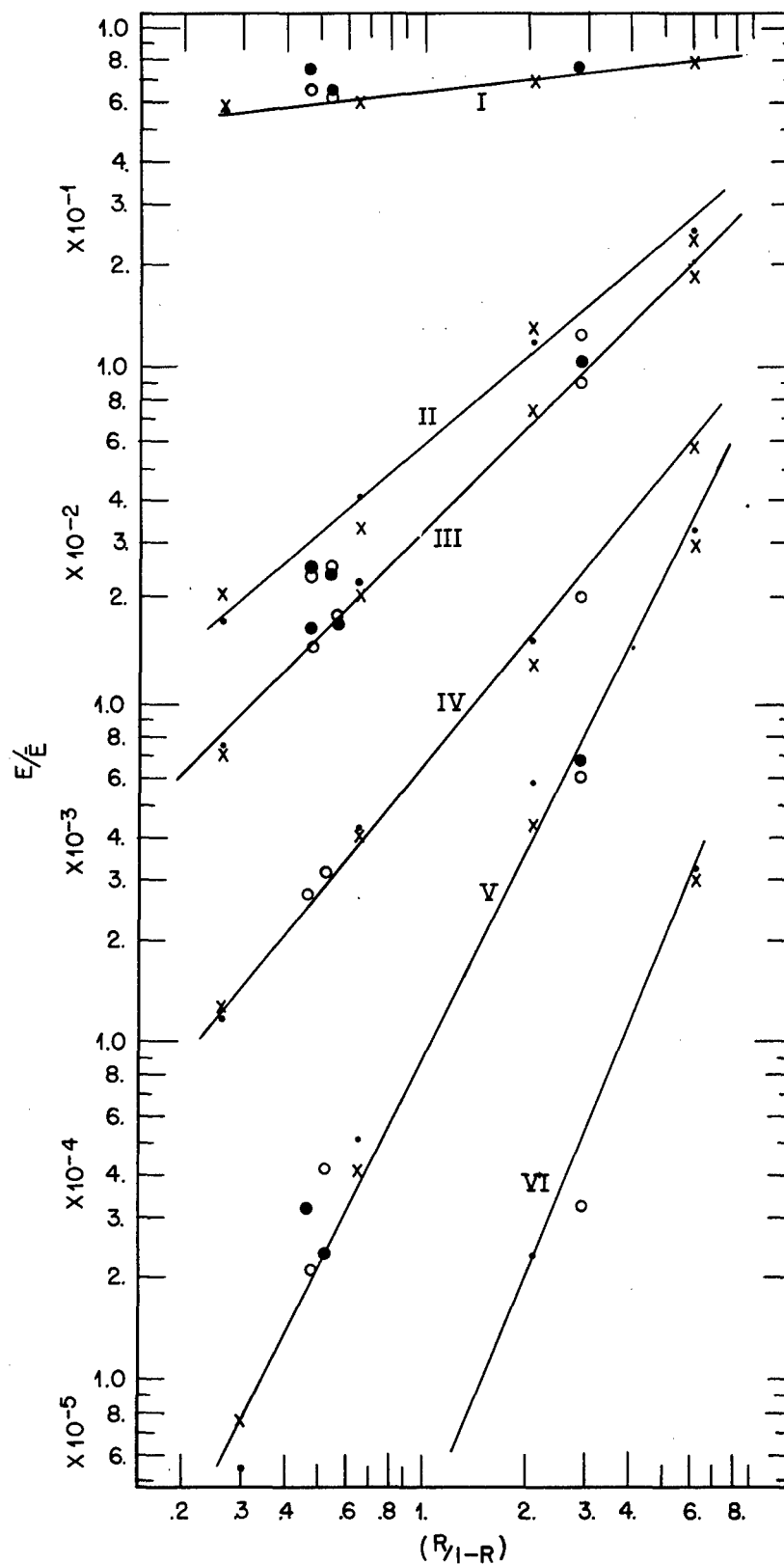


Fig. 4.2—Illuminance in the shelter as a function of the reflection factor (R) of the interior. I, head wall at system axis. II, head wall near ceiling. III, left wall—second stair well. IV, corridor wall—opposite last step. V, entrance to fast-fill room. VI, floor—center of fast-fill room. Model studies: ●, point source; x, extended source. Actual shelter: ○, photocell; ●, MacBeth.

spectral reflectance curves indicate that the grays were very neutral but that the buff had a high red reflectance. This may have reduced the accuracy of the data for that condition of shelter interior since the selectivity of reflectance made the measured illumination progressively redder going through the shelter.

TABLE 4.3—RATIOS OF ILLUMINANCE AT WALLS TO AVERAGE ILLUMINANCE
AT PLANE OF SHELTER APERTURE (MODEL STUDIES)

Location in model	$R/(1-R) = 6.2$	$R/(1-R) = 2.1$	$R/(1-R) = 0.65$	$R/(1-R) = 0.26$
Point source				
Head wall at intersection of system axis	7.89×10^{-1}	6.86×10^{-1}	5.99×10^{-1}	5.48×10^{-1}
Scattered light on head wall near ceiling	2.48×10^{-1}	1.18×10^{-1}	4.01×10^{-2}	1.72×10^{-2}
Wall at left of second stair well above 2nd tread	1.91×10^{-1}	7.25×10^{-2}	2.27×10^{-2}	7.34×10^{-3}
Wall at bottom of second stair well 1 ft above floor	6.08×10^{-2}	1.50×10^{-2}	4.18×10^{-3}	1.05×10^{-3}
Entrance to fast-fill room	3.23×10^{-2}	5.75×10^{-3}	5.06×10^{-4}	5.82×10^{-5}
Floor in center of fast-fill room	3.18×10^{-3}	2.22×10^{-4}		
Extended source				
Head wall at intersection of system axis	7.99×10^{-1}	6.83×10^{-1}	5.91×10^{-1}	5.01×10^{-1}
Scattered light on head wall near ceiling	2.53×10^{-1}	1.54×10^{-1}	5.13×10^{-2}	1.65×10^{-2}
Wall at left of second stair well above 2nd tread	1.85×10^{-1}	7.25×10^{-2}	2.07×10^{-2}	6.96×10^{-3}
Wall at bottom of second stair well 1 ft above floor	5.75×10^{-2}	1.27×10^{-2}	4.01×10^{-3}	1.25×10^{-3}
Entrance to fast-fill room	2.86×10^{-2}	4.20×10^{-3}	4.01×10^{-4}	7.38×10^{-5}
Floor in center of fast-fill room	2.97×10^{-3}			

4.6 MEASUREMENTS WITH SUNLIGHT

A complete set of measurements was made with the MacBeth Illuminometer on the buff-painted shelter with midday sunlight as the source. A 5-in. pointer was taped to the concrete in the center of the first stair well at the edge of the ceiling over the first landing. The position of the shadow of this pointer cast by the sun on the interior of the stair wells was recorded each time a measurement was made. From these data the polar and zenith angles of the sun could be computed for each time recorded. The illuminance in the plane of the shelter aperture was determined four times during the 1½ hours of the test. The measurements were started at 2 P.M., at which time the illuminance at the aperture was 7200 ft-c, compared with about 28 ft-c with the 2-kw lamp.

The results of the measurements made with sunlight are shown in Table 4.2. There is rough agreement with the results of the 2-kw lamp on the same buff paint, the values falling within a factor of 3 for the most part. The apparent reflection factor for the highly selective buff paint was probably much lower for the bluer sunlight but probably not as low as 0.62, which would yield the $R/(1-R)$ to give the same fit as the tungsten illumination. One source of difference is probably the reduced area of brightly illuminated walls acting as secondary sources.

Even with the spread in results, the daylight measurements served to generalize the measurements of the attenuation of light in the shelters. Under the stated limitation of static conditions, if the average irradiance on the aperture of the shelter can be predicted for any size fireball at any angle to, or any distance from, the shelter, the irradiance at any point in the shelter can be predicted to within a factor of 3.

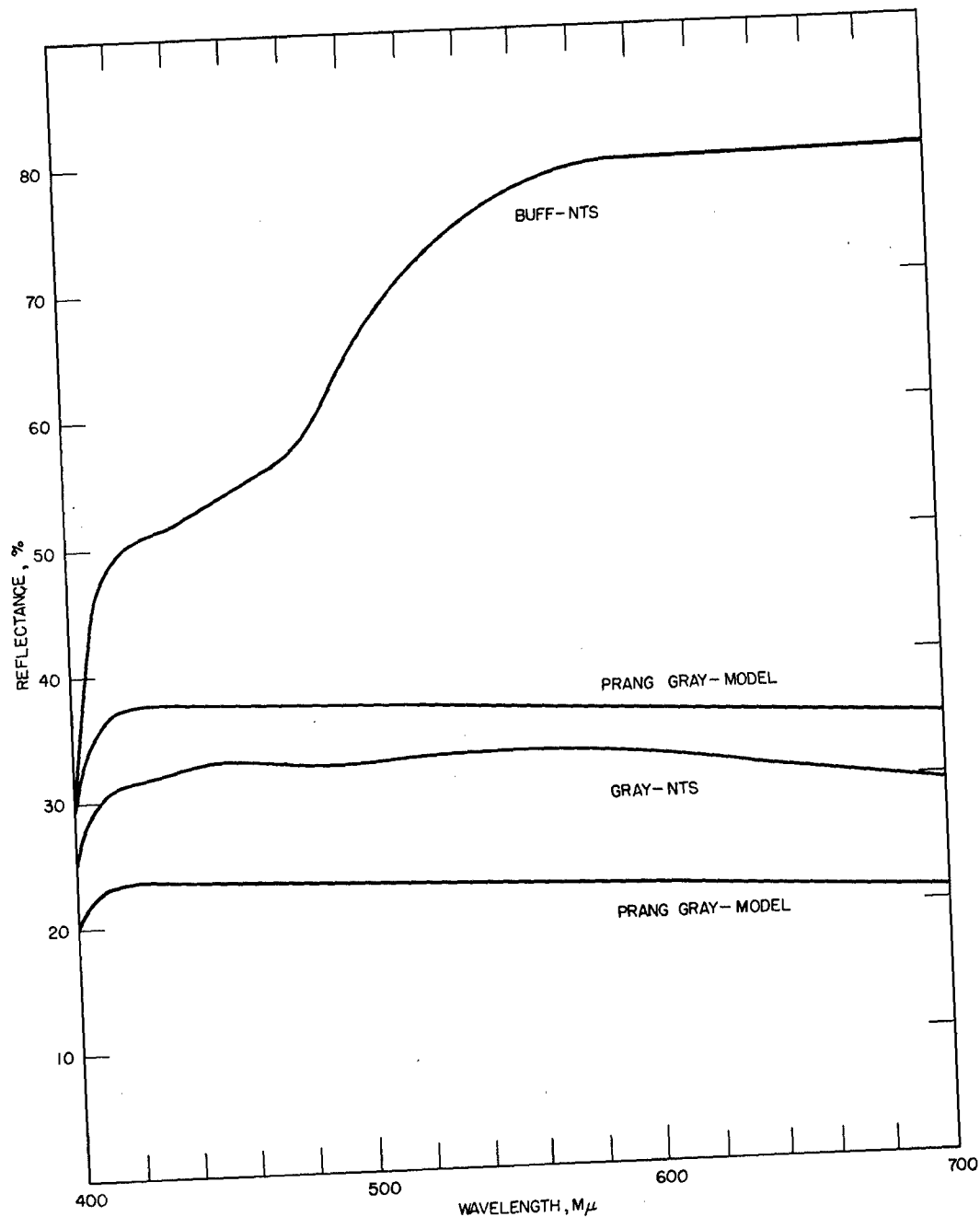


Fig. 4.3—Spectral reflectance of paints used in model studies and in field tests.

REFERENCES

1. T. P. Davis, L. J. Krolak, and J. A. Basso, A Tungsten Source Suitable for Producing Flash Burns, *J. Opt. Soc. Am.*, 45: 397 (1955).
2. M. E. Fogel and C. G. Fink, *Trans. Electrochem. Soc.*, 66: 271-319 (1934); N. R. Campbell and M. K. Freeth, *J. Sci. Instr.*, 11: 125 (1934); and L. A. Wood, *Rev. Sci. Instr.*, 7: 157 (1936).
3. L. J. Krolak, The Measurement of Diffuse Reflectance of Pig Skin, Titanium Dioxide Paint and India Ink; The Transmittance of Titanium Dioxide and India Ink, Report UR-439, April 1956.
4. J. A. Jacquez et al., Integrating Sphere for Measuring Diffuse Reflectance in the Near Infrared, *J. Opt. Soc. Am.*, 45: 781 (1955).

Chapter 5

CONCLUSIONS

Some animals located in open underground shelters at NTS during atomic weapon tests received burns from an unknown thermal source. This study was undertaken to determine whether or not thermal radiation could be ruled out as the cause of such burns. From the entryway transmission factors given above and from reasonably liberal estimates of the thermal radiation incident on the plane of the shelter entrance, it may be predicted that the radiant exposure of the animals was about $\frac{1}{200}$ of that required to produce the burns that were observed. Thus, on the basis of these static measurements, thermal radiation may be ruled out as an important causative agent of the observed burns in open underground shelters.

The excellent internal consistency of the results from the model studies and the agreement of these results with those from the field studies would lead to considerable confidence in this predicted exposure if it could be assumed that transient effects would not appreciably alter the transmission of radiation through the shelter entryway. However, the radiation on the walls of the shelter entryway from the thermal pulse of the weapon is great enough to heat the walls and the boundary layer of air to high temperatures within a fraction of a second. One possible effect of such heating would be to produce a varying index of refraction of the air in the entryway such that total internal reflection of the radiant energy within the air columns would occur. If this condition existed even imperfectly in the stair wells and corridor of the shelter and raised the effective wall reflectance to 80 per cent, the radiant exposure at the entrance to the fast-fill room would be increased to the value required to produce a burn comparable to those found on the animals. Another possible effect of the rapid heating of the entryway walls would be an explosive spalling of a thin surface layer of the concrete. This would fill the entryway with finely divided particles which could act as scattering centers to increase markedly the entryway transmission.

Although it was beyond the scope of these studies to attempt to quantify the transient effects, it is felt that the results of the static measurements provide strong evidence that radiant energy was neither the sole causative agent nor the most important such agent in producing the observed burns within the shelters. Hot winds and/or hot wind-borne dust are now considered to be the most likely agents.